Hindawi
International Journal of Photoenergy
Volume 2022, Article ID 6643133, 12 pages
https://doi.org/10.1155/2022/6643133

Research Article

In Situ LID and Regeneration of PERC Solar Cells from Different Positions of a B-Doped Cz-Si Ingot

Shuai Yuan,[1] **Siqi Ding**,[1] **Bin Ai**,[1] **Daming Chen**,[2] **Jingsheng Jin**,[3] **Jiaxing Ye**,[1] **Depeng Qiu**,[1] **Xiaopu Sun**,[4] **and Xueqin Liang**[5]

[1]*School of Materials Science and Engineering, Guangdong Provincial Key Laboratory of Photovoltaic Technologies, Sun Yat-sen University, Guangzhou 510006, China*
[2]*State Key Laboratory of PV Science and Technology, Trina Solar, Changzhou 213031, China*
[3]*Jinko Solar Holding Co. Ltd., Haining 314416, China*
[4]*CSG PVTECH Co., Ltd., Dongguan 523141, China*
[5]*Yichang CSG Polysilicon Co., Ltd., Yichang 443007, China*

Correspondence should be addressed to Bin Ai; stsab@mail.sysu.edu.cn

Received 20 October 2020; Revised 14 November 2021; Accepted 14 December 2021; Published 4 January 2022

Academic Editor: Ahmad Umar

In order to investigate the light-induced-degradation (LID) and regeneration of industrial PERC solar cells made from different positions of silicon wafers in a silicon ingot, five groups of silicon wafers were cut from a commercial solar-grade boron-doped Czochralski silicon (Cz-Si) ingot from top to bottom with a certain distance and made into PERC solar cells by using the standard industrial process after measuring lifetimes of minority carriers and concentrations of boron, oxygen, carbon, and transition metal impurities. Then, the changes of their I-V characteristic parameters (efficiency η, open-circuit voltage V_{oc}, short-circuit current I_{sc}, and fill factor FF) with time were in situ measured by using a solar cell I-V tester during the 1st LID (45°C, 1 sun, 12 h), regeneration (100°C, 1 sun, 24 h), and 2nd LID (45°C, 1 sun, 12 h). The results show that the LID and regeneration of the PERC solar cells are caused by the transition of B-O defects playing a dominant role together with the dissociation of Fe-B pairs playing a secondary role. The decay of η during the 1st LID is caused by the degradation of V_{oc}, I_{sc}, and FF, while the increase of η during the regeneration is mainly contributed by V_{oc} and FF, and the decay of η during the 2nd LID is mainly induced by the degradation of I_{sc}. After regeneration, the decay rate of η reduces from 4.43%–5.56% (relative) during the 1st LID to 0.33%–1.75% (relative) during the 2nd LID.

1. Introduction

Although boron-doped (B-doped) Czochralski silicon (Cz-Si) 11solar cells possess the advantages of low cost, high efficiency, and mature production technology, they also have a problem of light-induced degradation (LID) which restricts their development. It is generally accepted that boron-oxygen (B-O) defects formed under illumination are mainly responsible for the LID in minority carrier lifetime of B-doped Cz-Si wafers thus the electrical performance of solar cells based on the Si wafers [1–3]. Since specific composition of B-O defects is still unknown [1, 2] and B-O defects related LID (BO-LID) can bring about huge losses in power generation to customers [4], the investigations on the LID of boron-doped Cz-Si solar cells and its elimination are not only of great scientific research value but also of great practical significance [4]. In order to suppress BO-LID, many research works have been done. In 2006, Herguth et al. proposed a method called regeneration to alleviate the recombination activity of B-O defects by illumination at elevated temperatures [5]. After regeneration treatment, the electrical performance of B-doped Cz-Si solar cells can nearly be recovered, and especially, they possess an anti-LID ability under solar cell working conditions. Thereafter, effectiveness of the regeneration reaction of B-O defects has been confirmed in B-doped Cz-Si wafers [1, 2] and even in p-type compensated Cz-Si solar

cells [6], and the regeneration treatment has been regarded as an effective way to suppress or eliminate the LID of B-doped Cz-Si solar cells [4].

However, most experiments on BO-LID and regeneration effect were conducted on lifetime samples. In contrast, there are few reports on the LID and regeneration of B-doped Cz-Si solar cells especially the new type PERC solar cells. Just as Basnyat et al. from the National Renewable Energy Laboratory (NREL) noted in their paper in 2015, "although a great deal of information is available on B-O effects in silicon, LID in solar cell has not been understood fully. LID effect on crystalline silicon solar cells is studied by a small number of research groups, using comparatively small sets of samples. Even the results reported in literature show large diversity" [7]. Different from the structures of the lifetime samples, Cz-Si solar cells have multiple functional layers and interfaces, therefore, to what extent can the findings obtained on the lifetime samples be applied to Cz-Si solar cells remains unknown [8]; thus, it is necessary to directly study the LID and regeneration of B-doped Cz-Si solar cells especially the PERC solar cells. Herguth et al. and Fertig et al. [9, 10] first reported the LID and regeneration of the PERC solar cells in 2015. However, their research results were based on the prototype PERC solar cells prepared in laboratory, which cannot represent those of real industrialized PERC solar cells [11]. In 2018, Modanese et al. studied the effect of Cu-LID on the PERC solar cells and found that copper contamination and silicon wafer quality are the key factors affecting the degree of Cu-LID [12]. Herguth et al. investigated a LID phenomenon of unknown source in PERC solar cells in 2018, which is characterized by a slight loss in J_{sc}, a strong loss in V_{oc}, and a great loss in FF and efficiency. It was found that degradation of front contact resistance results in significant degradation of series resistance, and back-surface-related degradation can give a consistent explanation on the experimental results [13]. In 2019, Fertig et al. reported that regenerated PERC solar cells suffer a severe LID of 19.1% (relative value) after a prolonged dark annealing (150°C, 552 h); in contrast, the measured LID was only 5.6% (relative value) for the PERC solar cells fabricated without regeneration treatment [14]. In 2019, Helmich et al. reported that the regeneration rate constant of the B-O defects in PERC solar cells increases proportionally with the excess carrier concentration [15].

Although several research works have been done on the LID and regeneration of the PERC solar cells, much more research works are still needed to thoroughly understand the LID and regeneration of B-doped Cz-Si solar cells especially the PERC solar cells. Different from previous studies, this paper focuses on in situ investigation on the LID and regeneration of industrialized PERC solar cells fabricated by using the silicon wafers from different positions of a commercial B-doped Cz-Si ingot. The research results are helpful to clarify the effects of the silicon wafer positions and resultant impurity concentration difference on the LID and regeneration of the industrialized PERC solar cells.

2. Experiment

Five groups of 156.75 mm × 156.75 mm pseudosquare silicon wafers were cut from a commercial solar-grade B-doped Cz-Si ingot with a certain distance and were numbered group 1 to group 5 in order from the top to bottom. For each group of silicon wafers, the concentrations of transition metal impurities (iron, copper, and nickel) were measured by inductively coupled plasma mass spectrometer (ICP-MS), and the concentrations of interstitial oxygen and carbon were measured on 2 mm thick neighboring silicon wafers by a Fourier transform infrared (FTIR) spectrometer at room temperature according to ASTM F 121:1983 using a calibration factor of 2.45×10^{17}, while substitutional boron content was indirectly determined by measuring the resistivities of the wafers by using a four-probe tester after killing thermal donors using 650°C annealing in Ar for 2 h. After removing about 8 μm damaged layer on each side by using 20% KOH solution at 80°C and thermally growing about 5 nm SiO_2 film on each side at 760°C, the minority carrier lifetimes of the wafers were measured by a Semi-Lab WT-2000 lifetime tester. Then, five groups of silicon wafers were made into PERC solar cells by using the standard industrialized process, which includes removing the damaged layer and texturing by KOH solution, $POCl_3$ diffusion at 850°C to form an emitter about 85 Ω/□, removing phosphorosilicate glass (PSG) and back junction by HF/HNO_3 solution, depositing about 20 nm AlO_x/140 nm SiN_x passivation layer on the rear side by PECVD at 400°C, depositing about 80 nm SiN_x antireflection film on the front side by PECVD at 450°C, laser grooving on the back passivation layer to form electrical contact windows, screen printing the front and back electrodes, and final sintering with temperature up to 800°C. It should be mentioned that no regeneration treatment was performed on the as-prepared PERC solar cells, and the efficiencies of the PERC solar cells (cell area = 244.67 cm^2) were in the range of 20.3% to 20.8% at the STC condition (AM1.5 spectra, 1000 W/m^2, 25°C). It should be emphasized that the measured efficiencies are lower than the real values because the solar simulator was calibrated to output 1 sun light intensity but the shading loss caused by the five-row-probe cartridge above the tested solar cell sample was not taken into account.

Finally, the as-prepared PERC solar cells were treated by the first 12-hour LID (45°C, 1 sun), 24-hour regeneration (100°C, 1 sun), and the second 12-hour LID (45°C, 1 sun) in sequence on a IVT VS-6821M solar cell I-V tester. At the four time nodes (before the 1st LID, after the 1st LID, after regeneration, and after 2nd LID), we performed full-area LBIC scan on the PERC solar cells using 2 μm step by a SemiLab WT-2000 lifetime tester at room temperature. However, the LBIC mapping results are not shown in this paper as some of LBIC maps contain a large proportion of blank areas formed by void data points which may result from limitations of the instrument itself. Although the results obtained from LBIC scan including two-dimensional LBIC (light beam-induced current) mapping diagrams and DL (diffusion length) distribution diagram are unreliable and invalid and cannot be used for explaining our experimental results, LBIC scan step offered the conditions for formation of Fe-B pairs as the process was carried out in a dark box for about 2.5 h. Since the I-V characteristic

parameters (efficiency η, short-circuit current I_{sc}, open-circuit voltage V_{oc}, and fill factor FF) of the PERC solar cells were in situ measured by the VS-6821M solar cell I-V tester at regular time intervals (10 s in the first hour, 1 min from the 1st hour to the 3rd hour, and 5 min after the 3rd hour) during the 1st LID, regeneration, and 2nd LID processes, the in situ LID and regeneration curves of the I-V characteristic parameters of the PERC solar cells were obtained. According to the claim of the manufacturer (IVT Corporation of Singapore) of the VS-6821M I-V tester, the uncertainties of measurement results of I_{sc}, V_{oc}, FF, and η in the confidence level of 95.4% are 4.99%, 0.51%, 0.48%, and 5.00%, respectively.

3. Basic Knowledge about Solar Cell Device Physics

To facilitate discussion, we give a brief review on fundamentals of solar cell device physics. According to single diode model, the I-V characteristic equation of a solar cell can be expressed as [16]

$$I = I_{ph} - I_D - I_{sh} = I_{ph} - I_0\left[e^{\frac{q(V+IR_s)}{nkT}} - 1\right] - \frac{V + IR_s}{R_{sh}}, \quad (1)$$

where I and V are the current and voltage on the load, respectively; I_{ph} is the photogenerated current; I_D is the leakage (or dark) current through the diode; I_{sh} is the shunt current through the shunt resistance R_{sh}; I_0 is the reverse saturation current of the diode in the dark; q is the elementary charge; R_s is the series resistance; n is the ideality factor of the diode; k is the Boltzmann constant; and T is the device temperature. For a practical solar cell with finite dimensions, I_0 can be written as [17]

$$\begin{aligned} I_0 &= qAn_i^2\left(\frac{D_p}{L_pN_D}\bullet F_N + \frac{D_n}{L_nN_A}\bullet F_P\right) \\ &= qAN_cN_v\left(\frac{1}{N_D}\sqrt{\frac{D_p}{\tau_p}}\bullet F_N + \frac{1}{N_A}\sqrt{\frac{D_n}{\tau_n}}\bullet F_P\right)e^{-\left(E_g/kT\right)}, \end{aligned} \quad (2)$$

where

$$\begin{aligned} F_N &= \frac{S_p\bullet\cosh\left(W_N/L_p\right) + \left(D_p/L_p\right)\bullet\sinh\left(W_N/L_p\right)}{\left(D_p/L_p\right)\bullet\cosh\left(W_N/L_p\right) + S_p\bullet\sinh\left(W_N/L_p\right)}, \\ F_P &= \frac{S_n\bullet\cosh\left(W_P/L_n\right) + \left(D_n/L_n\right)\bullet\sinh\left(W_P/L_n\right)}{\left(D_n/L_n\right)\bullet\cosh\left(W_P/L_n\right) + S_n\bullet\sinh\left(W_P/L_n\right)}, \end{aligned} \quad (3)$$

where A is the cross-sectional area of the p-n junction; n_i and E_g are the intrinsic carrier concentration and band gap of the semiconductor material, respectively; D_p and D_n are the diffusion coefficients of holes and electrons, respectively; L_p and L_n are the diffusion lengths of holes and electrons as minority carriers, respectively; N_D and N_A are the donor and acceptor concentrations in the n region and p region, respectively; N_c and N_v are the effective density of states in the conduction band and valence band, respectively; τ_p and τ_n are the lifetimes of holes and electrons as minority carriers, respectively; S_p and S_n are the surface recombination velocities of the n region and p region, respectively; and W_N and W_P are the thickness of the n region and p region, respectively. Obviously, for our case, the reverse saturation current I_0 is mainly determined by the properties of silicon, the cross-sectional area of the p-n junction, thickness, surface recombination velocities, crystalline quality (τ_p, τ_n, L_p, and L_n), and doping concentration (N_D, N_A) of the n region and p region as well as temperature.

When a solar cell is at the short-circuit state, $V = 0$ and $I = I_{sc}$, the dark current I_D through the diode is very low and can be neglected; from equation (1), we have

$$I_{sc} = \frac{I_{ph}}{1 + (R_s/R_{sh})}. \quad (4)$$

For the general case, $R_{sh} >> R_s$; thus, $I_{sc} \approx I_{ph}$ holds.

When a solar cell is at the open-circuit state, $I = 0$ and $V = V_{oc}$, assuming that the R_{sh} is large enough so that the I_{sh} can be neglected, from equation (1), we have

$$V_{oc} = \frac{nkT}{q}\ln\left(\frac{I_{ph}}{I_0} + 1\right). \quad (5)$$

Fill factor FF is defined as the ratio of maximum power P_m output by a solar cell to the product of V_{oc} and I_{sc}, i.e.,

$$FF = \frac{P_m}{V_{oc}I_{sc}}. \quad (6)$$

For an ideal solar cell in which the effect of R_s and R_{sh} can be neglected, its fill factor FF_0 can be expressed by [17, 18]

$$FF_0 = \frac{v_{oc} - \ln\left(v_{oc} + 0.72\right)}{v_{oc} + 1}, \quad (7)$$

where v_{oc} is the dimensionless voltage $v_{oc} = qV_{oc}/nkT$. Equation (7) shows that the ideal fill factor FF_0 increases with the v_{oc}. After considering the effect of R_s and R_{sh}, the FF of a p-n junction solar cell can be given by [17, 18]

$$FF = FF_s\left[1 - \frac{(v_{oc} + 0.7)FF_s}{v_{oc}\bullet r_{sh}}\right]. \quad (8)$$

Here,

$$FF_s = FF_0\left[(1 - 1.1r_s) + \frac{r_s^2}{5.4}\right], \quad (9)$$

where FF_s is the fill factor of a solar cell in which only the effect of R_s is considered and r_s and r_{sh} are the normalized resistances, which are equal to R_s and R_{sh} divided by V_{oc}/I_{sc}, respectively. From equations (7)–(9), we can see that FF is affected by multiple factors such as R_s, R_{sh}, V_{oc}, n, I_0, and I_{sc}

in a complex way. To improve FF, one can decrease R_s and I_0 and increase R_{sh}, V_{oc}, and I_{sc} meanwhile.

Efficiency η is defined as the ratio of maximum power P_m output by a solar cell to the incident light power P_{in} on the device, i.e.,

$$\eta = \frac{P_m}{P_{in}} = \frac{V_{oc} \bullet I_{sc} \bullet FF}{P_{in}}. \quad (10)$$

Equation (10) shows that the η is determined by the product of V_{oc}, I_{sc}, and FF for the given incident light intensity and area of a solar cell.

4. Results and Discussion

4.1. Impurity Concentration and Lifetime of Silicon Wafers. Table 1 shows the measured lifetimes and resistivities as well as boron (B), oxygen (O), carbon (C), iron (Fe), copper (Cu), and nickel (Ni) contents of the five groups of silicon wafers. As shown in Table 1, from the top to bottom of the Cz-Si ingot, O content gradually decreases while B, C, Fe, Cu, and Ni contents gradually increase. With the increase of B content, the lifetime and resistivity gradually decrease. It should be mentioned that O content is approximately one order of magnitude higher than C content, two orders of magnitude higher than B content, three orders of magnitude higher than Fe content, and four orders of magnitude higher than Cu and Ni contents.

For the impurities such as B, C, Fe, Cu, and Ni, their distributions along the solidifying direction of the Cz-Si ingot are basically determined by their segregation coefficients in silicon; herein, the segregation coefficient is defined as the ratio of the solubility of the impurity in the solid phase at the liquid-solid-interface to the solubility in the liquid phase [19]. Since B, C, Fe, Cu, and Ni impurities all possess segregation coefficients less than 1 in silicon [19, 20], their contents gradually increase towards the tail of the Cz-Si ingot. For O impurity, its distribution along the solidifying direction of the Cz-Si ingot is determined not only by its segregation coefficient in silicon but also by the contact area between the quartz crucible and the silicon melt, and the latter may play a more important role because O impurities in the Cz-Si ingot mainly come from the dissolving quartz crucible wall under corrosion of the silicon melt at high temperature. As the growth proceeds, the contact area between the quartz crucible and the silicon melt is gradually reduced, which results in decreasing O incorporation in the silicon melt and thus decreasing O content towards the tail of the ingot [21]. Furthermore, this distribution is enhanced by the segregation coefficient of O which is larger than 1 [19]. Obviously, our test results on concentrations of the impurities can be given a good explanation from the point of view of impurity segregation and major origin of O. As compared with impurity distribution reported in Cz-Si, our O distribution along Cz-Si ingot is consistent with ref. [21] and our transition metal impurity distributions are in good agreement with ref. [22]. Since different groups of the Si wafers show little difference in C content and C content has little effect on lifetime of Cz-Si wafers [23], we will neglect the influence of C content on the LID and regeneration of the PERC solar cells in the following.

4.2. PERC Solar Cells. Figure 1 shows the in situ changes of the *I-V* characteristic parameters of five groups of PERC solar cells with time during the 1st LID (45°C, 1 sun, 12 h). As shown in Figure 1, η, I_{sc}, V_{oc}, and FF of most samples exhibit the typical characteristics of BO-LID, which is characterized by a double exponential decay corresponding to a "fast decay" and a "slow decay," respectively [2, 24]. Furthermore, P3 has the highest η and V_{oc}, whereas the bottom samples (P4 and P5) have larger LID in V_{oc}.

Under the condition of the 1st LID, the changes of R_s, R_{sh}, and surface passivation can be neglected, therefore, the decays of *I-V* characteristic parameters of the PERC solar cells are mainly caused by the LID of bulk minority carrier lifetime τ. For the as-prepared PERC solar cells, R_s is about 0.2 $\Omega \cdot cm^2$ while R_{sh} is above 2000 $\Omega \cdot cm^2$, which means $R_{sh} >> R_s$, thus, $I_{sc} \approx I_{ph}$ holds according to equation (4). It can be seen from equations (2)–(5) that the LID of the τ can result in the decrease of the collection efficiency thus decay of I_{sc} or I_{ph} on the one hand [25] and the increase of dark saturation current I_0 thus the decay of V_{oc} on the other hand. Furthermore, the decay of I_{ph} can also induce the degradation of V_{oc} according to equation (5). It is easily known from equations (7)–(9) that the decay of FF is mainly determined by that of V_{oc} when the changes of R_s and R_{sh} are neglected. From equation (10), the decay of η is the product of the decays of V_{oc}, I_{sc}, and FF. In a word, the degradations of V_{oc}, I_{sc}, FF, and η during the 1st LID result from the LID of τ, and degradation of τ under LID conditions has been reported by ref. [1, 3]. The larger LID in V_{oc} of bottom samples (P4 and P5) may result from their higher B and Fe contents. Ref. [26] has shown that the higher B content means the higher B-O defect concentration when the O content is in a range of 5.0×10^{17} cm^{-3} to 8.0×10^{17} cm^{-3}. In addition, the Coulomb attraction between Fe^+ and B^- reduces the efficiency of phosphorus diffusion gettering (PDG) [27], resulting in higher Fe-B pair concentration in the samples with higher B and Fe content, and the dissociation of Fe-B pairs would result in LID of most *I-V* characteristic parameters of a solar cell [28]. P3 has the highest η and V_{oc}, which may be related to its moderate B and O content and lower transition metal impurity content.

Figure 2 shows the in situ changes of the *I-V* characteristic parameters of five groups of PERC solar cells with time during the regeneration (100°C, 1 sun, 24 h). As shown in Figure 2, the η of P1-P5, V_{oc} of P3-P5, and FF of P2-P4 first decay then rise and finally reach saturation, with the extent of the rise much larger than the extent of the decay. Furthermore, the decay and rise extent in η, I_{sc}, and V_{oc} as well as the time required to reach saturation basically increases with B content. Different from above regeneration curves, the V_{oc} of P1-P2 and FF of P1 first rise linearly and then tend to reach saturation. In addition, the I_{sc} of P1-P3 first decreases, then increases, and finally decreases slowly, while the I_{sc} of P4-P5 first decreases, then increases, and finally tends to reach saturation.

We note that FF shows similar regeneration curves to V_{oc}, which implies that under our regeneration condition,

Table 1: The average values of lifetime, resistivity, and B, O, C, Fe, Cu, and Ni concentrations of five groups of Si wafers.

Group	Lifetime (μs)	Resistivity (Ω•cm)	B (atoms/cm^3)	O (atoms/cm^3)	C (atoms/cm^3)	Fe (atoms/cm^3)	Cu (atoms/cm^3)	Ni (atoms/cm^3)
1	27.60	1.79	$8.10E+15$	$9.65E+17$	$0.78E+17$	$3.25E+14$	$2.26E+13$	$1.07E+13$
2	24.19	1.78	$8.16E+15$	$8.53E+17$	$0.81E+17$	$3.40E+14$	$3.23E+13$	$1.12E+13$
3	24.17	1.49	$9.83E+15$	$7.51E+17$	$0.90E+17$	$3.44E+14$	$3.41E+13$	$1.23E+13$
4	22.95	1.29	$11.47E+15$	$7.24E+17$	$0.97E+17$	$4.47E+14$	$3.73E+13$	$1.36E+13$
5	21.57	1.16	$12.91E+15$	$6.43E+17$	$1.12E+17$	$5.39E+14$	$3.94E+13$	$1.68E+13$

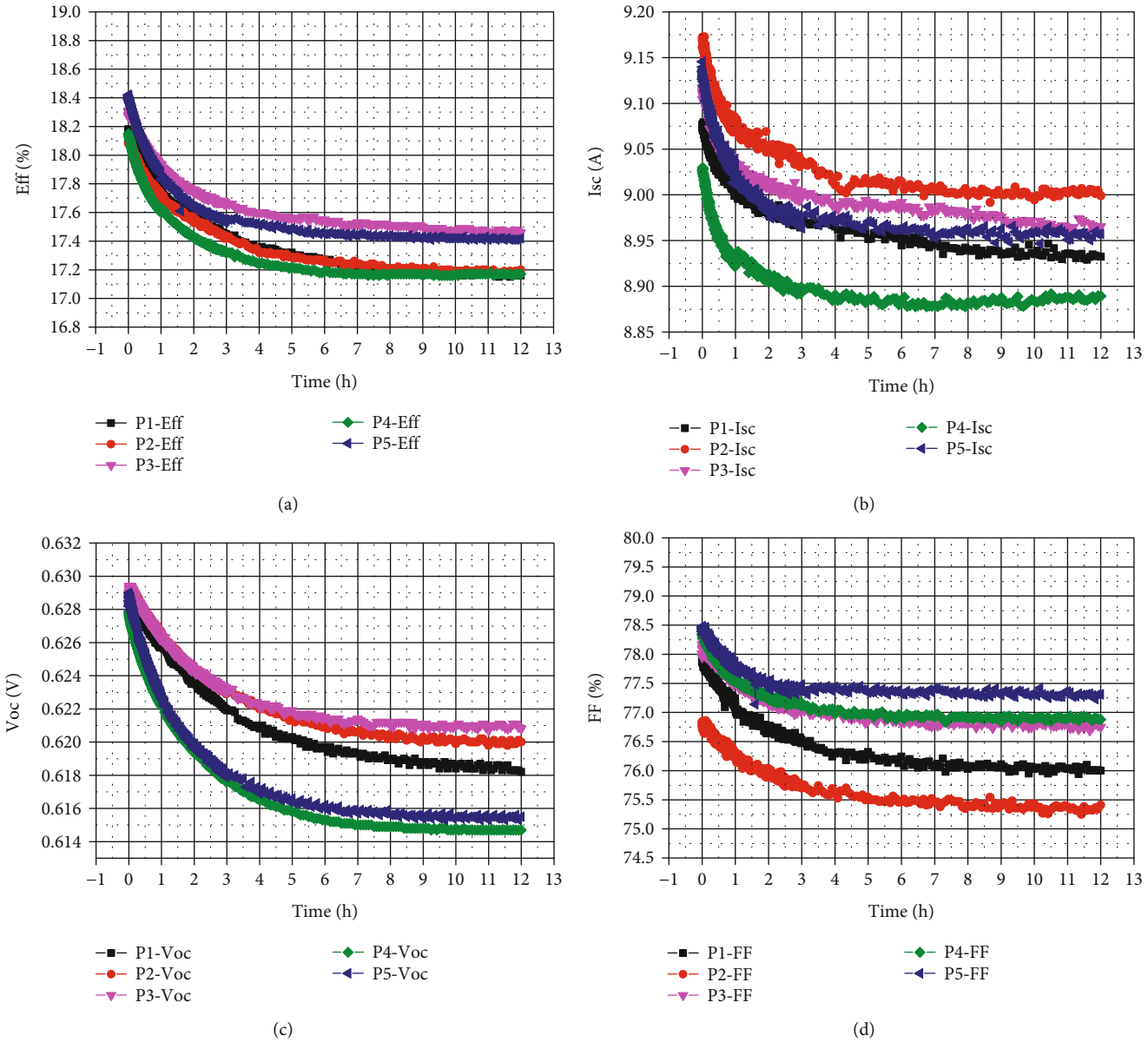

Figure 1: In situ variation of I-V characteristic parameters of five groups of PERC solar cells with time during the 1st LID (45°C, 1 sun, 12 h).

the change of FF is basically determined by that of V_{oc}, and the changes of R_s and R_{sh} can be neglected. In addition, η also shows a similar regeneration curves to V_{oc}, indicating that the change of η is also dominated by that of V_{oc}. In contrast, I_{sc} shows different regeneration curves from those of η, V_{oc}, and FF, with decreased I_{sc} values after the regeneration except P5. The reason why I_{sc} shows very different regeneration curves from V_{oc} is as follows: (1) the lifetimes limited by B-O defects or Fe-B pairs (or interstitial Fe ion Fe_i^+) are both injection dependent; however, V_{oc} and I_{sc} are measured

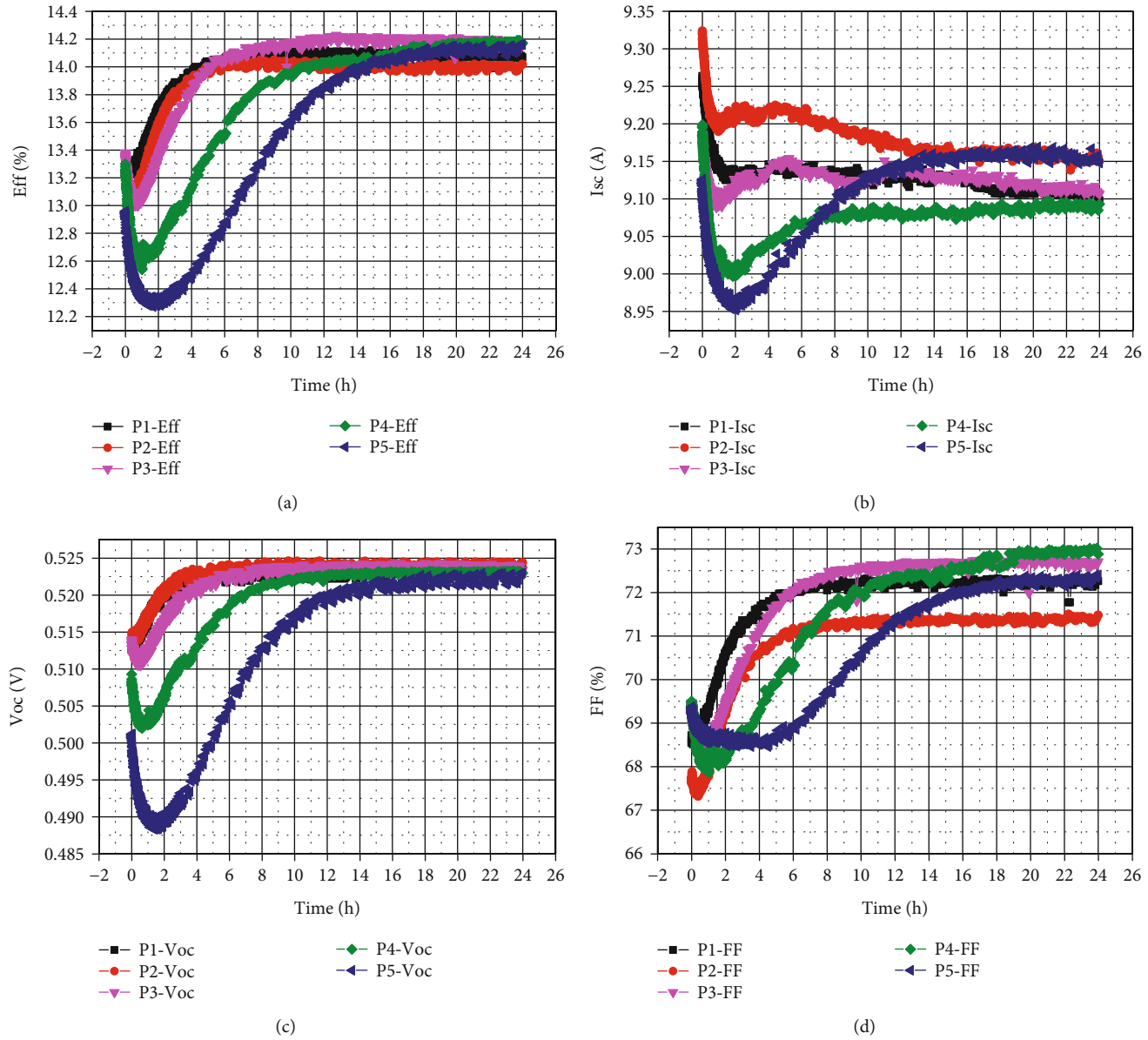

FIGURE 2: In situ variation of I-V characteristic parameters of five groups of PERC solar cells with time during the regeneration (100°C, 1 sun, 24 h).

at very different excess carrier concentrations (Δn), which results in the very different behavior of V_{oc} and I_{sc} [29]. Taking the dissociation of Fe-B pairs as an example, the recombination activities of a Fe-B pair and Fe_i^+ change with injection level of minority carriers. When the injection level is lower than excess carrier concentration corresponding to the crossover point (Δn_{COP}), the recombination activity of a Fe-B pair is lower than that of Fe_i^+, which means that dissociation of a Fe-B pair will result in LID of minority carrier lifetime τ; when the injection level is higher than Δn_{COP}, the recombination activity of a Fe-B pair is higher than that of a Fe_i^+, which means that dissociation of a Fe-B pair will give rise to photo-induced enhancement of τ [29]. The I_{sc} measured at injection levels always below the Δn_{COP} would degrade when FeB pairs dissociate, while the V_{oc} may decrease, or remain constant, or even increase, depending on the position of excess carrier concentration under open-circuit condition relative to Δn_{COP} [29]. (2) V_{oc} and I_{sc} have different dependencies on τ. Specifically speaking, I_{sc} is proportional to $\tau^{1/2}$, while V_{oc} is proportional to ln τ. That is to say, with the decrease of τ, I_{sc} decreases more remarkably than V_{oc}. In other words, I_{sc} is more sensitive to the change of τ than V_{oc}. (3) The further slow decay after the slow rise in I_{sc} of P1-P3 may result from the degradation of PECVD AlO_x/SiN_x rear passivation [13]. However, no further decay occurs in I_{sc} of P4-P5, which may be due to the higher B-O defect concentration of P4-P5 and the positive effect of B-O defect regeneration reaction on τ compensating the negative effect of back passivation degradation in P4-P5.

Interestingly, we note that at the initial stage of regeneration, the V_{oc} of P1-P2 increases directly, while the V_{oc} of P3-P5 first decreases and then increases, and the degradation and regeneration extents increase with increasing B and Fe contents. In order to explain the experimental phenomenon, we explore the three possibilities (BO-LID, LeTID, and dissociation of Fe-B pairs): (1) the degradation of V_{oc} at the initial stage of regeneration cannot be caused by B-O defects. After the 1st LID treatment (1 sun, 45°C, and 12 h), the B-O defects in PERC solar cells exist mainly in the form of degradation state. Because no dark annealing treatment above 100°C was performed on the samples before the regeneration, no B-O defects in annealed state were formed [30], and no BO-LID would occur at the initial stage of regeneration. (2) LeTID (Light and elevated Temperature-Induced Degradation) was also not involved in the degradation of V_{oc} at the initial stage of regeneration. Although there is still controversy about whether LeTID exists in B-doped Cz-Si [31, 32], the possibility of occurrence of LeTID in our samples has to be carefully examined. By using the method given by ref. [33] for judging whether the as-used illuminated annealing conditions can activate LeTID defects, we measured the IDLS (Injection-Dependent Lifetime Spectra) curves of five groups of lifetime samples made from same position of silicon wafers as five groups of PERC solar cells by using a WCT-120 equipment after sintering, dark annealing at 200°C for 30 min, and regeneration at 100°C and 1 sun for 24 h. It should be mentioned that the lifetime samples were prepared by the fabrication process of PERC solar cells without the steps of phosphorus diffusion, removing PSG, laser grooving on the back passivation layer, and screen printing front and back electrodes. In order to avoid the influence of Fe_i^+ on the measurement results, all the samples were kept in the dark at room temperature for 3 h before each of the IDLS measurements to make most of Fe_i^+ in the samples change into Fe-B pairs. The measurement results are shown in Figure 3. It can be seen from Figure 3 that the lifetimes of five groups of lifetime samples after the regeneration are all close to those after sintering and dark annealing at 200°C for 30 min, or even slightly higher than the latter two. This result illustrates that the LeTID defects generated in the Cz-Si samples by our regeneration treatment (100°C, 1 sun, and 24 h) can be neglected. (3) The degradation of V_{oc} at the initial stage of regeneration can be attributed to the dissociation of Fe-B pairs. According to ref. [28], the dissociation of Fe-B pairs into Fe_i^+ under illumination would lead to a degradation in most I-V characteristic parameters of crystalline silicon solar cells. In particular, I_{sc} and η always show a pronounced degradation, whereas the V_{oc} either decreases or keeps constant or even increases depending on Fe contamination levels. Our observed experimental phenomenon at the initial stage of regeneration can be well explained by ref. [28]. Specifically speaking, for P1-P2 with lower Fe content, V_{oc} keeps constant, while η, I_{sc}, and FF degrade. As a comparison, for P3-P5 with higher Fe content, all the I-V characteristic parameters degrade. In a word, the variation of I-V characteristic parameters of P1-P5 at the initial stage of regeneration can be well explained by the dissociation of Fe-B pairs. In addition, Fe-B pairs formed during 2.5 h LBIC scan before regeneration, together with the experimental results of the degradation extent increasing with B and Fe contents, further justify our judgement.

Figure 4 shows the in situ variation of the I-V characteristic parameters of five groups of PERC solar cells with time during the 2nd LID (45°C, 1 sun, 12 h). As shown in Figure 4, the η and I_{sc} of all the samples suffer a certain degradation at the early stage of the 2nd LID. In contrast, V_{oc} and FF of all the samples excluding the V_{oc} of P2 basically remain stable throughout the 2nd LID, and the V_{oc} of P5 as well as FF of P4 and P5 even show an upward trend.

At the early stage of the 2nd LID, the I_{sc} and η of all the samples suffer a degradation, while the V_{oc} either decreases or keeps constant or increases. After that, the I-V characteristic parameters of all the samples basically keep stable. Obviously, our experimental results observed at the early stage of the 2nd LID are in good accordance with the change features of the I-V characteristic parameters induced by dissociation of Fe-B pairs [28]. Since I_{sc} and V_{oc} are measured at very different excess carrier concentrations, the dissociation of Fe-B pairs always results in a pronounced degradation in I_{sc} and η, but different changes in V_{oc}, which either decreases or keeps constant or even increases, depending on the position of excess carrier concentration relative to Δn_{COP} [28]. During the 1st LID, the degradations of all the I-V characteristic parameters occur, which means that even the excess carrier concentration under open-circuit condition is still below the Δn_{COP} for each sample. However, the situation for the 2nd LID totally changes. Before the 2nd LID, the minority carrier lifetimes of all the samples were improved by regeneration treatment, and Fe-B pairs were formed during 2.5 h LBIC scan. According to the calculation formula of excess carrier concentration $\Delta n = G \cdot \tau$ and constant generation rate G corresponding to 1 sun light intensity for our case, the improved minority carrier lifetime τ means the increased Δn, and the increased Δn may approach to or even surpass the Δn_{COP}, leading to a constant V_{oc} or even increased V_{oc} due to dissociation of Fe-B pairs. Specifically speaking, the decreased, constant, and increased V_{oc} of P2, P3, and P5 indicate that the Δn of P2, P3, and P5 are below, near, and above the Δn_{COP}, respectively. In a word, the changes of I-V characteristic parameters of the PERC solar cells during the early stage of the 2nd LID can be given a good explanation by the dissociation of Fe-B pairs. It should be mentioned that no BO-LID would occur under the 2nd LID condition, because most of B-O defects in PERC solar cells have been converted into the stable regenerated state after the regeneration.

Figure 5 shows the relative changes of I-V characteristic parameters of five groups of PERC solar cells before and after each process. As shown in Figure 5, for all the samples the decrease of η during the 1st LID results from the decrease of V_{oc}, I_{sc}, and FF, while the increase of η during the regeneration is mainly contributed by V_{oc} and FF, and the decrease of η during the 2nd LID is mainly caused by the decrease of I_{sc}. During the 1st LID, the PERC solar cells made from top and bottom silicon wafers have larger decay in η and V_{oc} than those made from middle silicon wafers, and the decay rate of η is in the range of 4.43%–5.56% (relative). After the regeneration, all the samples have an increase in η, V_{oc}, and FF but

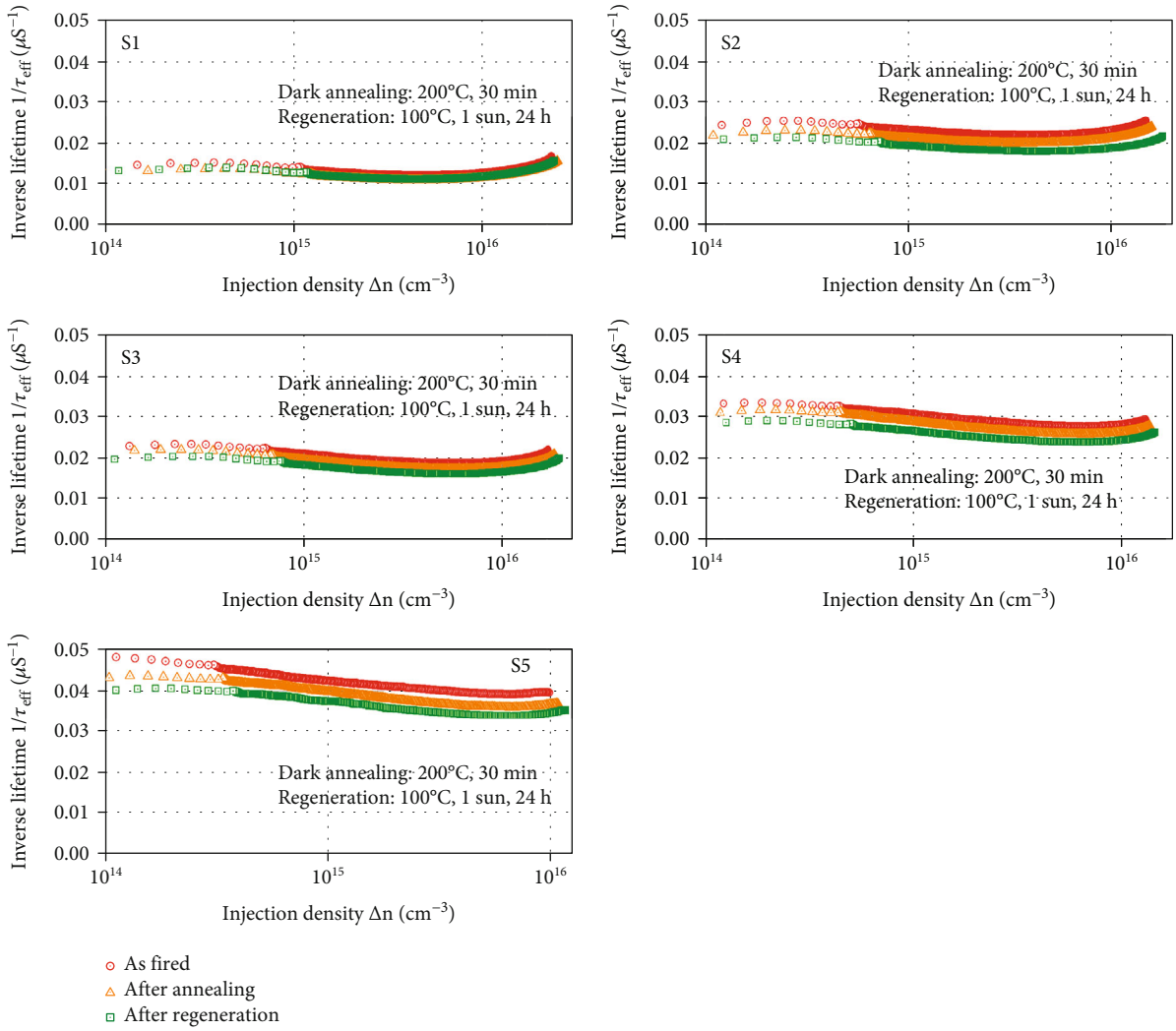

Figure 3: The IDLS spectra of five groups of lifetime samples corresponding to five groups of PERC solar cells measured after sintering, dark annealing at 200°C for 30 min, and regeneration at 100°C and 1 sun for 24 h.

suffer a decay in I_{sc} excluding P5. Furthermore, the rate of rise of η increases with B content, and it ranges from 5.71% to 9.26% (relative). In addition, generally, the higher the decay rates in V_{oc} and FF during the 1st LID, the higher the increase rates in V_{oc} and FF during the regeneration, which can be given a good explanation from the regeneration of B-O defects. During the 2nd LID, all the samples except P2 show a good stability in V_{oc} and FF but suffer a decay in η and I_{sc}. Moreover, the decay rates of η reduce to 0.33%–1.75% (relative). In addition, the relative change rates of V_{oc} and FF during the 2nd LID also decrease, which are two and one order of magnitude lower than those during the 1st LID, respectively.

Because all the Cz-Si wafers were made into PERC solar cells by using the same standard industrialized process, the difference in LID and regeneration of P1-P5 should be mainly caused by the difference in impurity concentration in as-used Cz-Si wafers. In fact, it can be seen from the impurity content that B-O defects and Fe-B pairs (or Fe_i^+) should be responsible for the observed LID and regeneration because of significantly higher O, B, and Fe contents in the base of as-prepared PERC solar cells. The reasons are as follows: (1) for all the Cz-Si wafers we used, the contents of B and O are far larger than those of transition metal impurities. As shown in Table 1, O content is about two orders of magnitude higher than B content, while the B content is at least one order of magnitude higher than Fe content and two orders of magnitude higher than Cu and Ni contents. It should be emphasized that O and B contents listed in Table 1 just correspond to the concentrations of interstitial O and substitutional B in the silicon wafers which are lower than practical O and B contents. In contrast, the contents of Fe, Cu, and Ni impurities shown in Table 1 are the total contents of them in various forms (interstitial state, substitutional state, complex, precipitation, etc.) in the silicon wafers, which are much higher than those of Fe, Cu, and Ni impurities with electrical activity. Therefore, the difference between the contents of B and O and those of transition metal impurities are much larger than those shown in

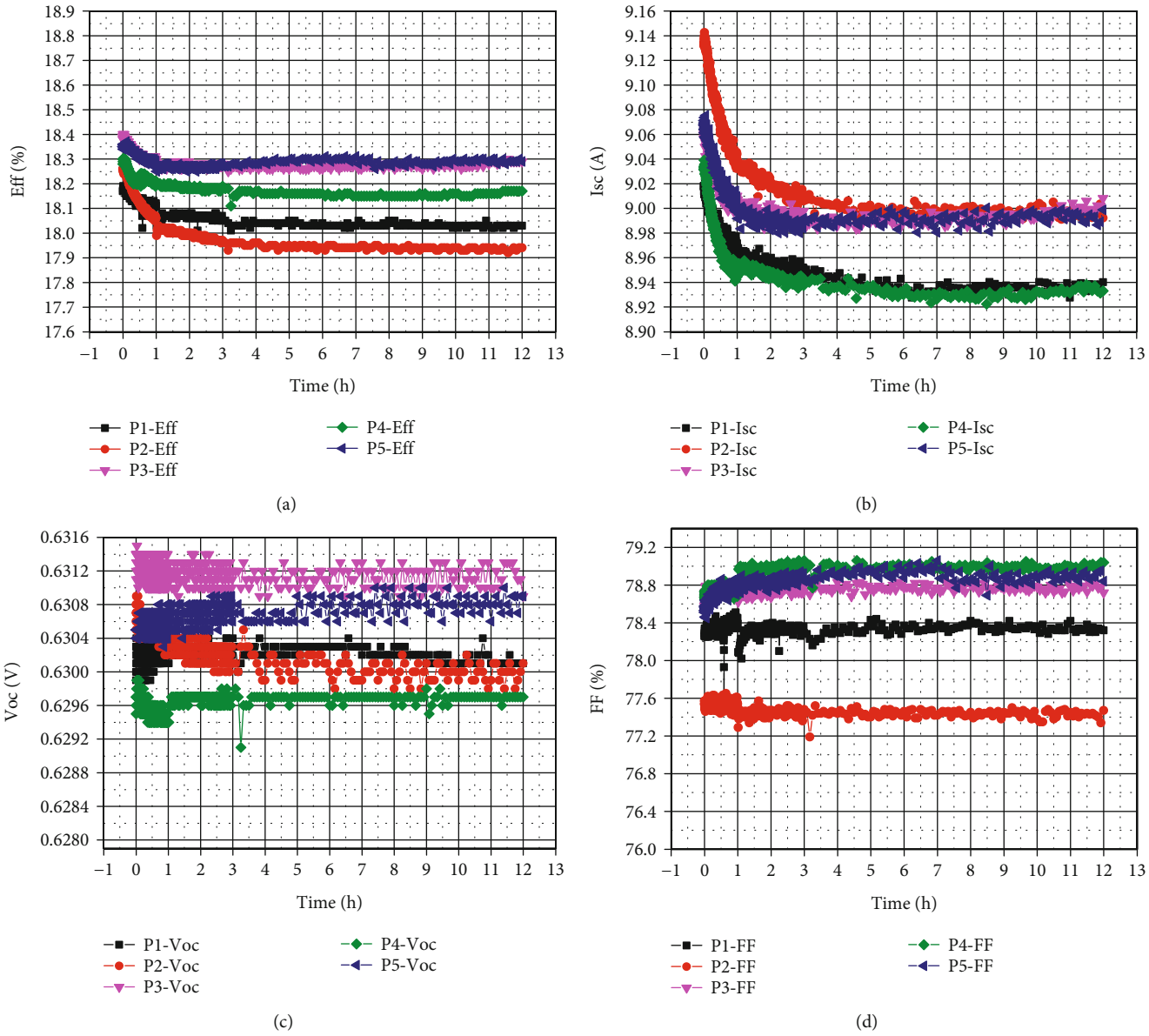

Figure 4: In situ variation of I-V characteristic parameters of five groups of PERC solar cells with time during the 2nd LID (45°C, 1 sun, 12 h).

Table 1. (2) After the phosphorus diffusion gettering (PDG) step included in the fabrication process of PERC solar cells, nearly all of Cu and Ni impurities can be removed from the silicon wafers excluding Fe impurities. The phosphorus diffusion condition we used is diffusion at 850°C for about 30 min, drive-in at 870°C for about 15 min, and total time of about 1.5 h for silicon wafers staying above 800°C. According to the empirical formulas given by ref. [34], we calculated the diffusion coefficients and the solubilities of Cu, Ni, and Fe impurities in silicon at 800°C, which are 4.49×10^{-5} cm^2/s, 1.24×10^{-5} cm^2/s, and 8.32×10^{-7} cm^2/s and 5.54×10^{16} atoms/cm^3, 1.58×10^{16} atoms/cm^3, and 2.84×10^{12} atoms/cm^3, respectively. As compared with the measured concentrations of Cu, Ni, and Fe ($<3.94 \times 10^{13}$, $<1.68 \times 10^{13}$, and $>3.25 \times 10^{14}$atoms/cm^3 for Cu, Ni, and Fe, respectively), Cu and Ni contents are much lower than their solubilities whereas Fe content is much higher than its solubility in silicon at 800°C, which means that Cu and Ni impurities can be completely dissolved while Fe impurity can only be partially dissolved in the silicon wafers at 800°C. Thus, Cu and Ni impurities can be effectively removed by PDG step due to their high diffusion coefficients and PDG gettering efficiency [27]. In contrast, partial dissolution and lower diffusion coefficient of Fe impurity together with lower gettering efficiency caused by Coulomb attraction between Fe^+ and B^- result in a part of Fe impurities remaining in the samples especially with higher B and Fe contents after PDG, which may exist in forms of Fe_i^+, Fe-B pairs, Fe precipitation, etc. The recombination activity of Fe precipitation can be neglected as compared with that of Fe_i^+ and Fe-B

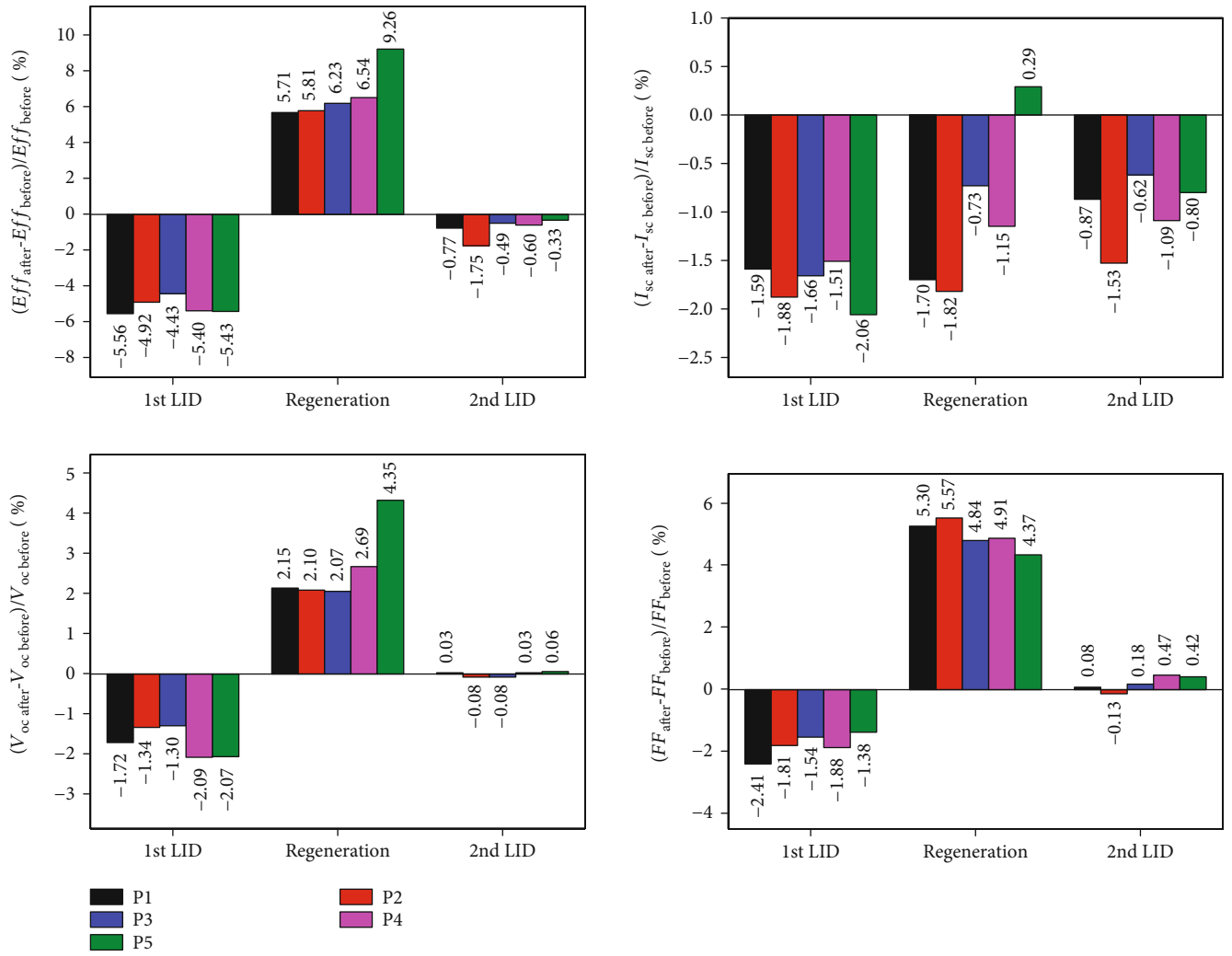

Figure 5: Relative changes of the I-V characteristic parameters of five groups of PERC solar cells before and after each process.

pairs, if they are formed by the same amount of Fe impurities [25]. (3) After the PDG and hydrogen passivation (sintering with SiN_x:H and AlO_x:H/SiN_x:H passivation layer) steps included in the fabrication process of PERC solar cells, the base minority carrier lifetime of as-prepared PERC solar cells can be significantly improved, which means that most of the defects caused by transition metal impurities can be effectively removed by PDG or passivated by hydrogen [25, 27]. However, whether Fe_i^+ or Fe-B can be effectively passivated by hydrogen remains controversial up to date [25].

In conclusion, the LID and regeneration of as-prepared PERC solar cells are caused by B-O defects and dissociation of Fe-B pairs. During the 1st LID, the decay of V_{oc}, I_{sc}, FF, and η results from B-O defects and dissociation of Fe-B pairs. The double exponential decay of I-V characteristic parameters of most samples suggests the dominance of BO-LID. During the regeneration, the initial change of the I-V characteristic parameters of the samples can be attributed to dissociation of Fe-B pairs, while the subsequent rise and saturation of the I-V characteristic parameters are caused by the regeneration of B-O defects. The extent of rise is much larger than the extent of decay, which indicates the dominant role of B-O defects. In addition, the further slow decay after the slow rise in I_{sc} of P1-P3 is ascribed to the slight rear passivation degradation. During the 2nd LID, the initial change of the I-V characteristic parameters of the samples is induced by the dissociation of Fe-B pairs. By comparing the 1st LID and 2nd LID, we can see that the extent of degradation caused by B-O defects is much larger than that by dissociation of Fe-B pairs. In addition, although P5 was fabricated by using the wafer with the highest B and Fe content, it nearly shows the largest decay and rise in η, V_{oc}, and I_{sc} during the 1st LID and the regeneration and minimum decay and highest value in η during the 2nd LID. This result further indicates that B-O defects dominate the LID and regeneration of as-prepared PERC solar cells. In a word, the LID and regeneration of the PERC solar cells result from B-O defects playing a dominant role and dissociation of Fe-B pairs playing a secondary role.

5. Conclusion

Five groups of silicon wafers cut from a solar grade Cz-silicon ingot from the top to bottom with a certain distance were made into PERC solar cells by using the standard industrial process; then, the as-prepared PERC solar cells were treated and in situ measured on a solar cell I-V tester by 1st LID (45°C, 1 sun, 12 h), regeneration (100°C, 1 sun, 24 h), and 2nd LID (45°C, 1 sun, 12 h). The results show that the LID and regeneration of I-V characteristic parameters of as-prepared PERC solar cells are mainly caused by B-O defects playing a dominant role and dissociation of Fe-B pairs playing a secondary role. Specifically, during the 1st LID, the decay of V_{oc}, I_{sc}, FF, and η is induced by B-O defects and dissociation of Fe-B pairs. During the regeneration, the initial change of the electrical parameters of the PERC solar cells can be attributed to dissociation of Fe-B pairs, while the subsequent rise and saturation of the electrical parameters result from the regeneration of B-O defects. During the 2nd LID, the initial change of the electrical parameters of the PERC solar cells is ascribed to dissociation of Fe-B pairs. Moreover, the decay of η during the 1st LID is caused by the degradation of V_{oc}, I_{sc}, and FF, while the increase of η during the regeneration is mainly contributed by V_{oc} and FF, and the decay of η during the 2nd LID is mainly induced by the decrease of I_{sc}. After regeneration, the decay rate of η reduces from 4.43%–5.56% (relative) during the 1st LID to 0.33%–1.75% (relative) during the 2nd LID.

Data Availability

The data used to support the findings of this study are included within the paper.

Conflicts of Interest

The authors declare no conflict of interests.

Authors' Contributions

Shuai Yuan and Siqi Ding performed experimental investigation and wrote the original draft; Bin Ai designed the experiments, analyzed the results, and revised the draft; Jiaxing Ye and Depeng Qiu discussed the experimental results; Xueqin Liang, Daming Chen, Jingsheng Jin, and Xiaopu Sun offered lots of help in preparing silicon wafers, lifetime samples, and PERC solar cells, respectively, Shuai Yuan and Siqi Ding are co-first authors.

Acknowledgments

This work was supported by the National Natural Science Foundation of China (Grant No. 61774171). The authors gratefully acknowledge this support.

References

[1] T. Niewelt, J. Schön, W. Warta, S. W. Glunz, and M. C. Schubert, "Degradation of crystalline silicon due to boron–oxygen defects," *IEEE Journal of Photovoltaics*, vol. 7, no. 1, pp. 383–398, 2017.

[2] J. Lindroos and H. Savin, "Review of light-induced degradation in crystalline silicon solar cells," *Solar Energy Materials and Solar Cells*, vol. 147, pp. 115–126, 2016.

[3] J. Schmidt, "Light-induced degradation in crystalline silicon solar cells," *Solid State Phenomena*, vol. 95-96, pp. 187–196, 2003.

[4] B. Hallam, A. Herguth, P. Hamer et al., "Eliminating light-induced degradation in commercial p-type Czochralski silicon solar cells," *Applied Sciences*, vol. 8, no. 1, p. 10, 2018.

[5] A. Herguth, G. Schubert, M. Kaes, and G. Hahn, "Avoiding boron-oxygen related degradation in highly boron doped Cz silicon," in *Proceedings of the 21st European Photovoltaic Solar Energy Conference and Exhibition (EUPVSEC)*, pp. 530–537, Dresden, Germany, 2006.

[6] C. Xiao, X. Yu, D. Yang, and D. Que, "Study on permanent deactivation of the light-induced degradation in p-type compensated crystalline silicon solar cells," *Solar Energy Materials and Solar Cells*, vol. 117, pp. 29–33, 2013.

[7] P. Basnyat, B. Sopori, S. Devayajanam et al., "Experimental study to separate surface and bulk contributions of light-induced degradation in crystalline silicon solar cells," *Emerging Materials Research*, vol. 4, no. 2, pp. 239–246, 2015.

[8] A. Herguth, S. Wilking, R. Horbelt, S. Ebert, C. D. F. Beckh, and G. Hahn, "Accelerating boron-oxygen related regeneration: lessons learned from the BORNEO project," in *Proceedings of the 31th European Photovoltaic Solar Energy Conference and Exhibition (EUPVSEC)*pp. 804–807, Hamburg, Germany, 2015.

[9] A. Herguth, R. Horbelt, S. Wilking, R. Job, and G. Hahn, "Comparison of BO regeneration dynamics in PERC and Al-BSF solar cells," *Energy Procedia*, vol. 77, pp. 75–82, 2015.

[10] F. Fertig, K. Krauß, and S. Rein, "Light-induced degradation of PECVD aluminium oxide passivated silicon solar cells," *Physica Status Solidi RRL*, vol. 9, no. 1, pp. 41–46, 2015.

[11] J. Ye, B. Ai, J. Jin, D. Qiu, R. Liang, and H. Shen, "Study on the electrical injection regeneration of industrialized B-doped Czochralski silicon PERC solar cells," *International Journal of Photoenergy*, vol. 2019, Article ID 5357370, 2019.

[12] C. Modanese, M. Wagner, F. Wolny et al., "Impact of copper on light-induced degradation in Czochralski silicon PERC solar cells," *Solar Energy Materials and Solar Cells*, vol. 186, pp. 373–377, 2018.

[13] A. Herguth, C. Derricks, and D. Sperber, "A detailed study on light-induced degradation of Cz-Si PERC-type solar cells: evidence of rear surface-related degradation," *IEEE Journal of Photovoltaics*, vol. 8, no. 5, pp. 1190–1201, 2018.

[14] F. Fertig, R. Lantzsch, F. Frühauf et al., "Excessive light-induced degradation in boron-doped Cz silicon PERC triggered by dark annealing," *Solar Energy Materials and Solar Cells*, vol. 200, p. 109968, 2019.

[15] L. Helmich, D. C. Walter, and J. Schmidt, "Direct examination of the deactivation of the boron–oxygen center in Cz-Si solar cells under regeneration conditions via electroluminescence," *IEEE Journal of Photovoltaics*, vol. 9, no. 6, pp. 1472–1476, 2019.

[16] D. T. Cotfas, P. A. Cotfas, and S. Kaplanis, "Methods to determine the dc parameters of solar cells: a critical review," *Renewable and Sustainable Energy Reviews*, vol. 28, pp. 588–596, 2013.

[17] M. A. Green, *Solar Cells: Operating Principles, Technology, and System Applications*, Prentice-Hall, 1981.

[18] B. Qi and J. Wang, "Fill factor in organic solar cells," *Physical Chemistry Chemical Physics*, vol. 15, no. 23, pp. 8972–8982, 2013.

[19] S. Wolf and R. N. Tauber, *Silicon processing for the VLSI era, Volume 1: process technology*, Lattice press, CA, 1986.

[20] P. Li, S. Ren, D. Jiang, J. Li, L. Zhang, and Y. Tan, "Effect of alternating magnetic field on the removal of metal impurities in silicon ingot by directional solidification," *Journal of Crystal Growth*, vol. 437, pp. 14–19, 2016.

[21] M. Wagner, F. Wolny, M. Hentsche et al., "Correlation of the LeTID amplitude to the aluminium bulk concentration and oxygen precipitation in PERC solar cells," *Solar Energy Materials and Solar Cells*, vol. 187, pp. 176–188, 2018.

[22] M. B. Shabani, T. Yamashita, and E. Morita, "Metallic impurities in mono and multi-crystalline silicon and their gettering by phosphorus diffusion," *ECS Transactions*, vol. 16, pp. 179–193, 2009.

[23] Y. Miyamura, H. Harada, S. Nakano, S. Nishizawa, and K. Kakimoto, "Relationship between carbon concentration and carrier lifetime in CZ-Si crystals," *Journal of Crystal Growth*, vol. 486, pp. 56–59, 2018.

[24] H. Hashigami, Y. Itakura, and T. Saitoh, "Effect of illumination conditions on Czochralski-grown silicon solar cell degradation," *Journal of Applied Physics*, vol. 93, no. 7, pp. 4240–4245, 2003.

[25] E. B. Yakimov, "Metal impurities and gettering in crystalline silicon," in *Handbook of Photovoltaic Silicon*, D. Yang, Ed., Springer-Verlag GmbH, Germany, 2019.

[26] S. Rein, S. Diez, R. Falster, and S. W. Glunz, "Quantitative correlation of the metastable defect in Cz-silicon with different impurities," in *Proceedings of the 3rd World Conference on Photovoltaic Energy Conversion*, pp. 1048–1052, Osaka, Japan, 2003.

[27] M. B. Shabani, T. Yamashita, and E. Morita, "Study of gettering mechanisms in silicon: competitive gettering between phosphorus diffusion gettering and other gettering sites," *Solid State Phenomena*, vol. 131-133, pp. 399–404, 2008.

[28] J. Schmidt, "Effect of dissociation of iron–boron pairs in crystalline silicon on solar cell properties," *Progress in Photovoltaics: Research and Applications*, vol. 13, no. 4, pp. 325–331, 2005.

[29] J. Schmidt, K. Bothe, D. Macdonald, J. Adey, R. Jones, and D. W. Palmer, "Electronically stimulated degradation of silicon solar cells," *Journal of Materials Research*, vol. 21, no. 1, pp. 5–12, 2006.

[30] A. Herguth, C. Derricks, and G. Hahn, "Regeneration of boron-oxygen related degradation in Cz-Si PERC-type solar cells at high temperatures," in *Proceedings of the 33rd European Photovoltaic Solar Energy Conference and Exhibition*, pp. 557–560, München, Germany, 2017.

[31] D. Chen, M. Kim, B. V. Stefani et al., "Evidence of an identical firing-activated carrier-induced defect in monocrystalline and multicrystalline silicon," *Solar Energy Materials and Solar Cells*, vol. 172, pp. 293–300, 2017.

[32] M. Winter, D. Walter, D. Bredemeier, and J. Schmidt, "Light-induced lifetime degradation effects at elevated temperature in Czochralski-grown silicon beyond boron-oxygen-related degradation," *Solar Energy Materials and Solar Cells*, vol. 201, 2019.

[33] D. Lin, Z. Hu, Q. He, D. Yang, L. Song, and X. Yu, "New insights on LeTID/BO-LID in p-type mono-crystalline silicon," *Solar Energy Materials & Solar Cells*, vol. 226, p. 111085, 2021.

[34] E. R. Weber, "Transition metals in silicon," *Applied Physics A*, vol. 30, no. 1, pp. 1–22, 1983.